WATER RESOURCES RESEARCH, VOL. 31, NO. 9, PAGES 2141–2157, SEPTEMBER 1995

Observation and three-dimensional simulation of chloride plumes in a sandy aquifer under forced-gradient conditions

T.-C. Jim Yeh,[1] J. Mas-Pla,[2] T. M. Williams,[3] and J. F. McCarthy[4]

Abstract. Two-well, forced-gradient tracer experiments over a distance of 5 m were carried out in a coastal sandy aquifer at Georgetown, South Carolina. The evolution of three-dimensional chloride plumes during two tracer experiments was observed. A three-dimensional finite element model for flow and transport was used with extensive hydraulic conductivity data obtained from slug tests to assess our ability to predict solute transport in the aquifer. Results showed that our predictive ability is limited to the bulk behavior of the plumes, which is mainly controlled by some "significant" heterogeneities. In addition, hydraulic conductivity values estimated by the Hvorslev method for analysis of slug tests best represented the hydraulic conductivity distribution of the sandy aquifer. Finally, the results of a long-term experiment illustrate the importance of temporal variability in boundary conditions in the prediction of solute transport in aquifers.

Introduction

Two-well, forced-gradient tracer experiments (one in May 1992, and the other in August-September, 1992) involving the injection of chloride and natural organic matter (NOM) were carried out in a coastal sandy aquifer at Georgetown, South Carolina. The ultimate goal of the experiments was to understand the mechanisms controlling the mobility and migration of NOM in the field and subsequently to improve our predictive ability (J. F. McCarthy et al., Field tracer tests on the mobility of natural organic matter and chloride in a sandy aquifer, 1, Field site description and failure of a simplified one-dimensional approach, submitted to *Water Resources Research*, 1994; hereinafter McCarthy et al. (submitted manuscript, 1994)). Since the mobility of NOM is controlled by both hydrological and chemical factors in the field, it becomes necessary to isolate the former from the latter in the transport process to understand the reaction between NOM and aquifer materials. Verification of our understanding of and ability to predict the groundwater flow regime under field conditions also becomes an essential step toward accomplishing the goal of our research.

It is well known that the groundwater flow regime is directly influenced by the spatial distribution of the hydraulic conductivity and that aquifers are inherently heterogeneous. However, attempts to address the heterogeneity issue were not made until the last decade. Since then, numerous stochastic approaches have been developed to deal with heterogeneities in the prediction of flow and solute transport in aquifers. An overview of these stochastic approaches can be found in the literature [e.g., *Yeh*, 1992; *Gelhar*, 1993]. Among these approaches, the effective (equivalent homogeneous) approach along with macrodispersion concept [*Gelhar and Axness*, 1983; *Dagan*, 1987] is attractive because of its simplicity and practicality. Several well-instrumented field sites at scales of tens and hundreds of meters were established, and many natural gradient tracer experiments have been conducted in the past few years to test the macrodispersion approach [e.g., *Freyberg*, 1986; *Sudicky*, 1986; *Garabedian et al.*, 1991; *Rehfeldt et al.*, 1992; *Jensen et al.*, 1993]. Overall, this approach has been found satisfactory for reproducing spatial moments of the plume after it has been displaced a distance much larger than the scale of heterogeneity. For shorter distances this approach is considered inadequate owing to limitations of the ergodicity assumption embedded in the macrodispersion concept.

The alternative approach to predict flow and solute transport in heterogeneous aquifers is to use a numerical simulation with high-resolution information on the spatial distribution of hydrologic properties of the aquifer (i.e., heterogeneous approach). Such a heterogeneous approach has, however, seldom been tested because it requires a detailed description of hydrologic properties of the aquifer. Tailored to testing the validity of the macrodispersion concept, the past natural gradient field experiments collected data on a large number of hydraulic properties at locations adjacent to the tracer experiments but not from within the paths of the tracer plume. As a result, these conductivity data sets are not useful for testing the heterogeneous approach, and verification of this approach under field conditions is clearly needed.

On the other hand, small-scale field tracer tests (such as two-well, forced-gradient tests over a distance of a few meters) have been the standard field method for studying hydrodynamic and chemical behaviors of contaminants or chemicals in the aquifer. Most analyses of these tests have relied on the assumption of aquifer homogeneity. Little attention had been given to the effect of heterogeneities until *Pickens and Grisak* [1981] demonstrated the scale dependence of macrodispersion in forced-gradient field experiments.

The performance of two-well tracer tests over a distance of 80 m in a sandy aquifer was investigated by *Molz et al.* [1986,

[1]Department of Hydrology and Water Resources, University of Arizona, Tucson.
[2]Unitat de Geodinàmica Externa i Hidrogeologia, Departamento de Geologia, Universitat Autònoma de Barcelona, Bellaterra, Spain.
[3]College of Forest and Recreation Resources, Belle W. Baruch Forest Science Institute, Clemson University, Georgetown, South Carolina.
[4]Environmental Science Division, Oak Ridge National Laboratory, Oak Ridge, Tennessee.

Paper number 95WR01947.
0043-1397/95/95WR-01947$05.00

Table 1. Mean and Variance of ln K at Each Depth

Layer	Depth, m	Number of Data*	Hvorslev		Cooper et al.	
			Mean	Variance	Mean	Variance
1	1.15	17 (11)	−11.75	0.41	−12.97	2.12
2	1.30	17 (13)	−11.83	0.44	−12.77	1.16
3	1.45	21 (18)	−11.88	0.44	−13.21	1.60
4	1.60	25 (22)	−11.87	0.61	−13.03	3.49
5	1.75	24 (22)	−11.69	0.73	−12.43	3.66
6	1.90	25 (23)	−11.32	1.01	−11.98	3.61
7	2.05	23 (24)	−11.28	0.81	−12.29	3.64
8	2.20	24	−10.56	0.96	−10.84	5.09
9	2.35	24	−10.24	0.92	−10.31	5.12
10	2.50	25	−9.72	0.59	−9.18	3.46
11	2.65	23	−9.48	0.28	−8.77	1.82

K was originally given in meters per second.
*Numbers in parentheses indicate the number of data points for the Cooper et al. method.

1988], *Huyakorn et al.* [1986], and *Güven et al.* [1992]. Hydraulic conductivity data in the vertical direction at 14 different locations between the injection and withdrawal wells were collected. Using the conductivity data set, tracer breakthroughs at sampling wells, and three-dimensional simulations, they concluded that the concentration breakthrough at the withdrawal well can be reasonably predicted if sufficient information on the spatial distribution of hydraulic conductivity is available, especially in the vertical direction. However, they reported difficulty in reproducing breakthroughs observed at different levels in a multilevel sampling well between the injection and the pumping wells.

Mas-Pla et al. [1992] showed that porosity values estimated from a two-well forced-gradient test using models assuming aquifer homogeneity were physically unrealistic. Moreover, McCarthy et al. (submitted manuscript, 1994) reported that even at very short distances (1.5 m), observed breakthrough curves of chloride and NOM at multilevel sampling wells could not be reproduced using a simple layered aquifer model with the knowledge of vertical conductivity distribution. As a result, they suggested that a detailed characterization of the three-dimensional hydraulic conductivity distribution is needed to understand the flow regime and, thus, to properly interpret the results of two-well tracer tests.

The overall objective of this paper is to describe the detailed groundwater flow regime at the tracer experiment site and our attempt to use the heterogeneous approach to model chloride movement in the experiments in 1992. To facilitate the heterogeneous approach, 308 slug tests were conducted to characterize the three-dimensional hydraulic conductivity distribution of the aquifer at the field site of this study. Analysis of the slug test data [*Mas-Pla*, 1993] revealed the complex nature of the hydraulic conductivity distribution in the sandy aquifer, which appears to explain the failure of the attempt by *Mas-Pla et al.* [1992] and McCarthy et al. (submitted manuscript, 1994) and suggests a fully three-dimensional numerical simulation. As a result, our first objective was to use this extensive collection of hydraulic conductivity data in a deterministic, three-dimensional numerical model to predict chloride tracer movement in the experiments. Success in the prediction of the tracer plume using such a three-dimensional heterogeneous approach may lead to better interpretation of the mechanism controlling the mobility of NOM under field conditions.

Although 308 slug tests were employed to characterize the field site, different methods of analyzing the slug test data resulted in significantly different hydraulic conductivity values [*Mas-Pla*, 1993]. For example, Table 1 shows the differences in means and variances of the natural log of hydraulic conductivity values at the field site, calculated from *Hvorslev*'s [1951] method and the method by *Cooper et al.* [1967]. Such a dilemma compels us to ask, Which conductivity value set is the most representative of the aquifer since both methods involve different simplifications? *Mas-Pla* [1993] suggested that the hydraulic conductivity values derived from the Hvorslev method seemed most reasonable. However, the definitive answer to this question lies in the ability of each conductivity value set to reproduce the observed evolution of tracer distributions. The second objective of this study was, therefore, to evaluate the usefulness of the two different conductivity value sets (i.e., one derived based on the Hvorslev method and the other based on the method of Cooper et al.) by numerical simulations of the observed three-dimensional chloride plume distributions during the tracer experiment conducted in May 1992.

Also this paper attempts to address a pragmatic but important sampling issue: How detailed a site characterization is necessary in order to adequately predict the migration of contaminants in aquifers? In other words, can a three-dimensional, layered approach ignoring the detailed distribution of heterogeneities within layers predict the behavior of the chloride plume adequately so that the effort of collecting a detailed three-dimensional hydraulic conductivity distribution can be reduced?

Finally, we tested what we learned in the chloride tracer experiment of May 1992 by predicting the migration of the chloride plume in the aquifer of the tracer injection experiment during August and September 1992, where NOM was also injected. Results of the NOM experiment are given by J. F. McCarthy et al. (Field tracer tests on the mobility of natural organic matter and chloride in a sandy aquifer, 4, Transport of natural organic matter, submitted to *Water Resources Research*, 1994).

Description of Field Experiments

A detailed description of the field site is presented in the papers by *Williams and McCarthy* [1991] and McCarthy et al. (submitted manuscript, 1994). The Georgetown site is in a coastal, sandy aquifer approximately 3 m thick, with distinct stratification, and bounded by an impervious clay layer at its

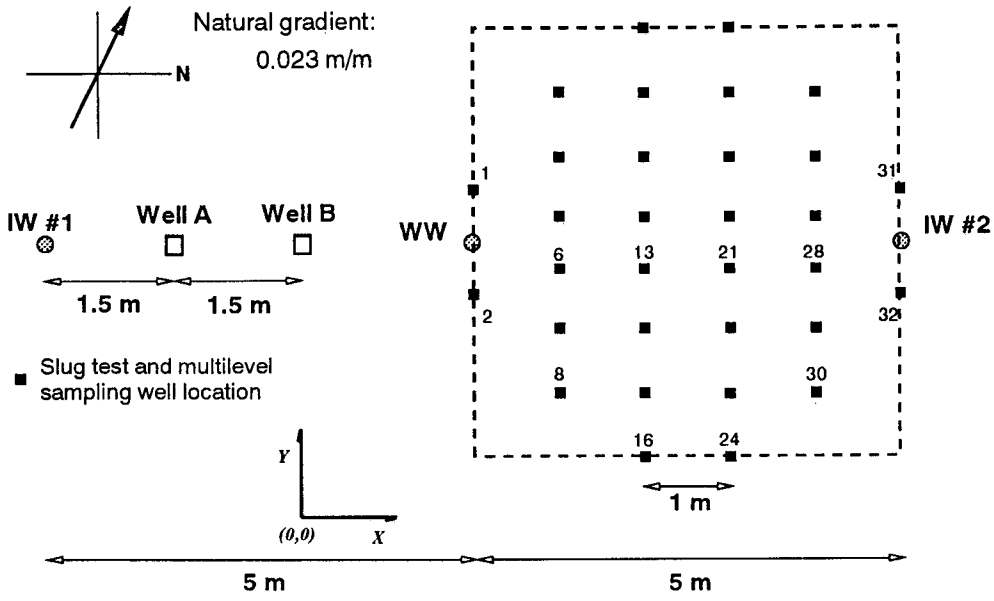

Figure 1. Well distribution pattern at the Georgetown site. IW 1: injection well used in the May 1990 test (McCarthy et al., submitted manuscript, 1994); IW 2: injection well used in the May 1992 and August-September 1992 tests; WW: withdrawal well.

bottom. In general, the upper layer consists of a fine, loamy sand with some clay (9% by weight) and some roots. Below this layer exists a zone of gleyed sand with a 4% clay content, which includes most of the saturated thickness of the aquifer. The deepest part of the aquifer is a layer of medium-coarse sand, consisting of clear quartz with a clay content less than 2%, and ranging from 0.15 to 0.30 m thick. The water table is approximately 1 m below ground level.

Thirty-two sampling wells were installed over a 5 × 5 m area between the withdrawal well (WW) and the injection well (IW 2) (Figure 1). Each well consisted of a 2.54-cm diameter polyvinyl chloride (PVC) pipe, fully screened from 1 m below the surface to the bottom of the aquifer. These wells were installed by manually driving the screens into the aquifer. After well development by pumping and gentle surging, falling head slug tests were conducted at eleven 15-cm depth intervals in each well. Because of sampling failures (primarily sand locking of packers and screen), only 308 time-drawdown curves were collected and analyzed for hydraulic conductivity by the techniques of *Hvorslev* [1951] and *Cooper et al.* [1967]. Results of the analysis of the slug tests are given by J. Mas-Pla et al. (Slug test analysis and aquifer heterogeneity, submitted to *Ground Water*, 1995; hereinafter Mas-Pla et al., submitted manuscript, 1995). Following the slug tests, a new set of packers were installed at each of the 28 remaining wells, which isolated five 15-cm intervals centered at depths of 1.4, 1.7, 2.0, 2.3, and 2.6 m below the land surface. Each packed interval was connected to the surface by a 2-mm Teflon microtube. Also shown in Figure 1 is the position of this experiment in relation to wells A and B, and the injection well (IW 1) developed for the May 1990 experiment (McCarthy et al., submitted manuscript, 1994).

Two tracer experiments were conducted during May 1992, and August-September 1992, respectively. Figures 2a–2c illustrate the variations in rainfall, and estimated regional groundwater hydraulic gradients and their orientations at the experimental site during the time span from April 27 through October 1, 1992. The first experiment (May 1992) involved an injection of a chloride tracer (KCl) at a concentration level of approximately 230 mg/L for 16 hours (Figure 3a) at IW 2 after a steady state flow regime had been reached under a constant injection and withdrawal rate of 3.78 L/min at the IW 2 and WW wells. During the entire 12 days of the test, samples were simultaneously collected from the five depths of the 28 monitoring wells to obtain a three-dimensional spatial distribution or "snapshots" of the chloride plume. To collect the tracer sample, groundwater was simultaneously extracted from all depths of a group of five wells, with an approximate rate of 100 mL/min, starting from the five locations closest to the injection well. The complete operation of sampling the entire array of wells took less than 20 min; therefore each snapshot can be considered instantaneous. Snapshots were taken every 2 hours during the first 30 hours, at 4- to 5-hour intervals until 100 hours and at longer intervals until the end of the experiment. A continuous breakthrough curve was also recorded at the withdrawal well. The chloride concentration of each sample was analyzed using the automated ferricyanide method [*Greenberg et al.*, 1985].

The second injection experiment took place during August-September 1992 at the same experimental site. This experiment was designed to test NOM chemistry mechanisms found in the 1990 experiments (McCarthy et al., submitted manuscript, 1994). The experiment ran for a period of 43 days with an injection period of 659 hours. Rather than being mixed with the NOM solution in the tank, chloride was metered into the injection stream with a target final concentration of 100 mg/L. Problems with the metering pump resulted in a fluctuating chloride concentration from 50 to 250 mg/L during the injection (Figure 3b). Further complicating this experiment, several heavy rainstorms occurred during the first 20 days of injection (Figure 2a). A higher regional water table limited the injection rate to 3.0 L/m. Because of the higher regional water table, a withdrawal rate of 4.5 L/m was needed to maintain the same gradient from the injection to withdrawal wells as was used in

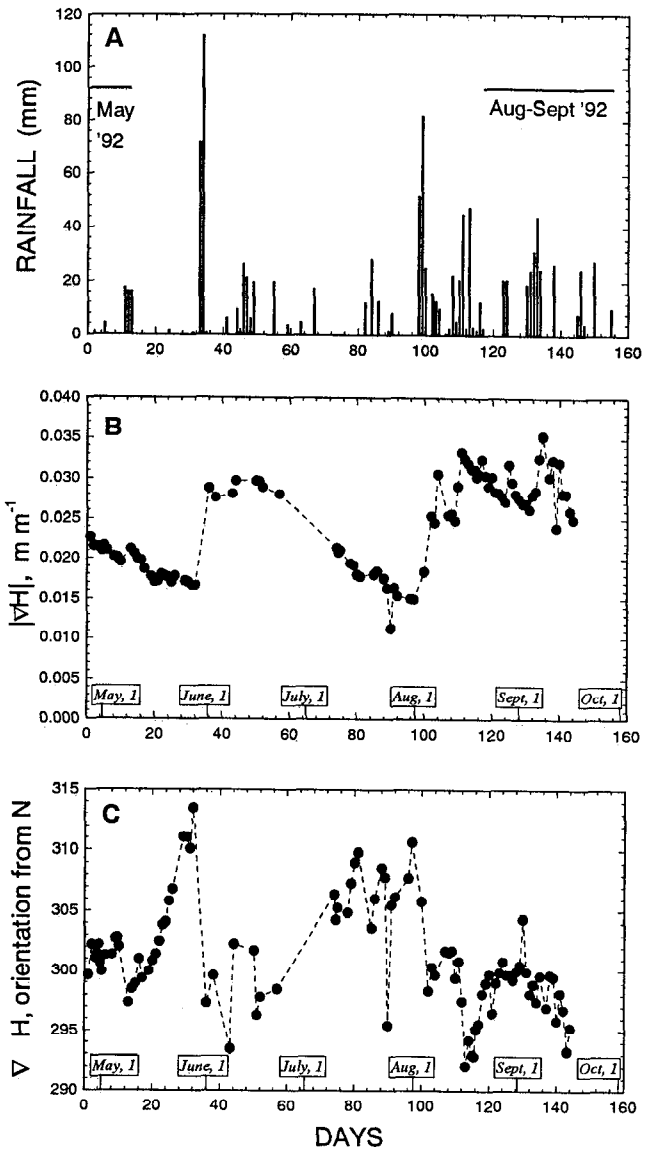

Figure 2. (a) Rainfall events measured at the Baruch Science Forestry Institute, Georgetown, South Carolina, (b) variations in natural groundwater hydraulic gradient magnitude, and (c) orientation during the period April 27 to October 1, 1992, at the Georgetown site.

the May experiment. Additionally, water was withdrawn from the well (IW 1) to intercept regional groundwater moving toward the withdrawal well. The rate of pumping in well (IW 1) varied with the regional water table from a high of 5.5 L/m (the capacity of the well) after heavy rain to 0 after a week without rain. Drawdown of this well was monitored in wells A and B and adjusted to try to maintain a steady state at the boundary of the modeled domain described later. Figure 4 depicts the injection and pumping rates at those wells during the entire test period.

Eighteen concentration snapshots were taken with variable intervals focusing on the early times of the experiment and the times following the shutdown of the tracer injection. Continuous breakthrough data were also collected at the withdrawal well and at 2.6 m depth in four sampling wells (wells 6, 13, 21, and 28) along the line between the injection and the withdrawal wells.

Modeling Approach

Numerical Model

A three-dimensional finite element model (MMOC3 [*Srivastava and Yeh*, 1992]) for water flow and transport of a chemically nonreactive or reactive solute under variably saturated conditions in porous media was used to simulate the observed three-dimensional plumes. MMOC3 solves the following equation describing the three-dimensional flow of water in a heterogeneous saturated porous media:

$$\frac{\partial}{\partial x_i}\left(K_{ij}\frac{\partial h}{\partial x_j}\right) = S_s\frac{\partial h}{\partial t} \tag{1}$$

where h is the hydraulic head, K_{ij} is the hydraulic conductivity tensor, S_s is the specific storage, x_i are the spatial coordinates (i = 1, 2, 3), and t is time. In our tracer experiments, flow is considered to be steady state; thus the right-hand side storage term becomes zero.

For transport of nonreactive solutes in the aquifer, MMOC3 solves the classical three-dimensional convection-dispersion equation:

$$\frac{\partial}{\partial x_i}\left(D_{ij}\frac{\partial C}{\partial x_j}\right) - v_i\frac{\partial C}{\partial x_i} = \frac{\partial C}{\partial t} \tag{2}$$

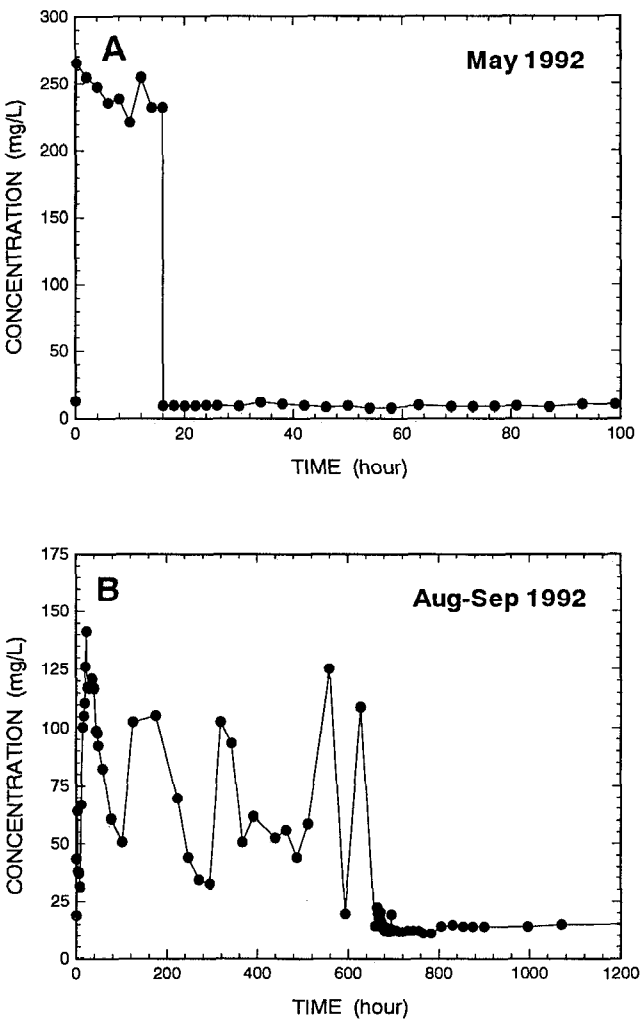

Figure 3. Chloride input concentrations during the May 1992 and the August-September 1992 tracer tests.

where C is the concentration of the tracer in units of mass per unit volume and v_i is the velocity component in the i direction. D_{ij} is the ij component of the hydrodynamic dispersion tensor which is calculated on the basis

$$D_{ij} = (\alpha_L - \alpha_T)\frac{q_i q_j}{q} + \alpha_T \delta_{ij} \quad (3)$$

where α_L and α_T are the local longitudinal and transverse dispersivity, respectively, which represent the effect of velocity variation smaller than the scale at which the hydraulic conductivity is defined. Here q is the magnitude of the specific discharge with components q_i.

Because of the importance of velocity on the simulation of solute transport, a continuous three-dimensional velocity field is obtained by application of the Galerkin technique to Darcy's law in MMOC3. The advective part of the transport equation is then solved in MMOC3 with a one-step backward particle-tracking technique, while the dispersive part is solved by the regular Galerkin finite element technique. *Srivastava and Yeh* [1992] and *Yeh et al.* [1993] demonstrated the robustness of this approach under a variety of flow scenarios. However, they also reported the problem of numerical dispersion associated with this approach.

To apply MMOC3 to the simulation of the tracer experiments, the simulation domain ($9 \times 7 \times 1.5$ m) was discretized into small, rectangular, prismatic elements as shown in Figure 5. Different element sizes were considered in order to accommodate the converging and diverging flow field created by the injection and withdrawal wells. Elements with $\Delta x = \Delta y = 0.1$ m and $\Delta z = 0.075$ m were used to represent the wells. The horizontal dimension of the element size was gradually increased up to 0.5 m near the boundaries, while the vertical dimension was kept the same at one-half the distance between the hydraulic conductivity measurements in the vertical direction. Such a discretization results in a finite element mesh of $27 \times 20 \times 23$ nodes and 10,868 variable-size elements. During the simulation of solute transport the maximum time step size was set to 3 min to ensure the accuracy of the numerical simulation.

Modeling Approach of May 1992 Injection Experiment

Two modeling approaches were employed to simulate the May 1992 chloride tracer experiment, namely, the heterogeneous and layered approaches. For both approaches the following boundary conditions were used in the simulations.

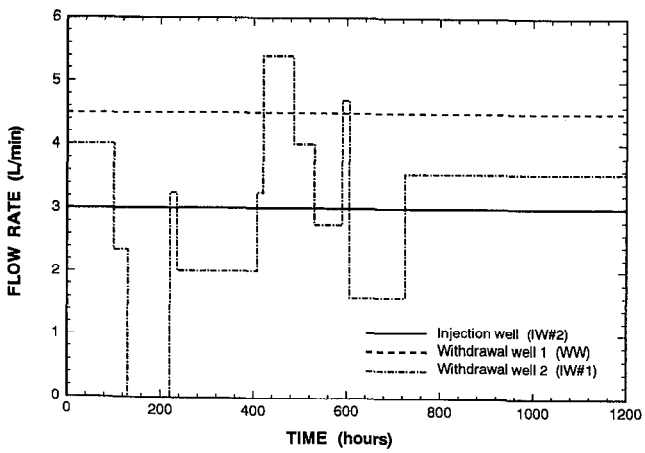

Figure 4. Variations of injection and withdrawal rates at the three active wells during the August-September 1992 tracer test (see text for explanation).

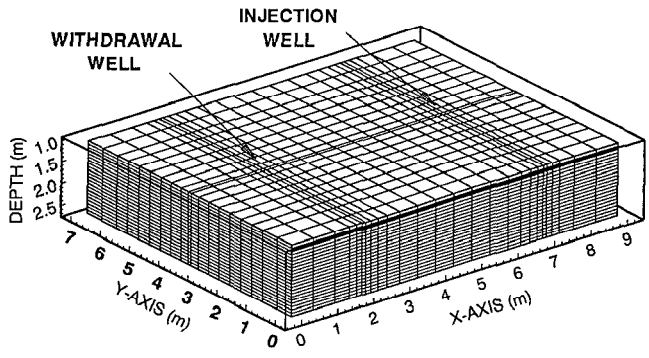

Figure 5. Three-dimensional view of the finite element mesh used in the numerical model.

No-flow boundary conditions were defined for the top and bottom boundaries of the simulation domain. Constant head values were assigned to the lateral boundaries. These head values were estimated using the analytical solution of Theis' equation for the well doublet, accounting for the average natural hydraulic gradient (0.023 m/m) of the site during the experiment (see Figures 1 and 3). Nodes representing the injection and withdrawal wells were also treated as constant head boundaries, with a constant head value throughout the entire depth. The head values at the wells were initially determined by the Theis equation but were adjusted so that the total fluxes at the injection and withdrawal wells calculated by the flow model matched with measured values.

For solute transport simulation, all nodes were assigned an initial chloride concentration of 11 mg/L, corresponding to the mean background concentration. Boundary nodes located in the half of the simulation domain that included the injection well were treated as no-dispersive flux boundary nodes. The boundary nodes in the other half of the domain that included the withdrawal well were defined as constant concentration nodes with the background concentration of groundwater. A time-variant concentration boundary condition was assigned to the nodes corresponding to the injection well to reflect the variation of the input concentration.

Heterogeneous approach. The hydrologic heterogeneity of the field site was incorporated into the model by assigning a different hydraulic conductivity value to each element. Since the number of elements used in the simulation is greater than the number of conductivity values collected, an interpolation/extrapolation scheme based on the inverse distance weight of the eight measurements nearest to the geometric center of each element was used. In addition, the vertical search radius of the interpolation scheme was restricted to one slug test interval as suggested by the geologic logs to preserve the layered structure of the aquifer. Using such an interpolation scheme and the conductivity value sets derived from the Hvorslev method and the method of Cooper et al., two different hydraulic conductivity fields were subsequently created (denoted hereinafter as the H and C conductivity value sets for the Hvorslev and the Cooper et al. methods, respectively). Figure 6 shows a three-dimensional view of the hydraulic conductivity distribution (based on the H conductivity value set) at the experimental site.

An average porosity of 0.25 was selected for the entire sandy

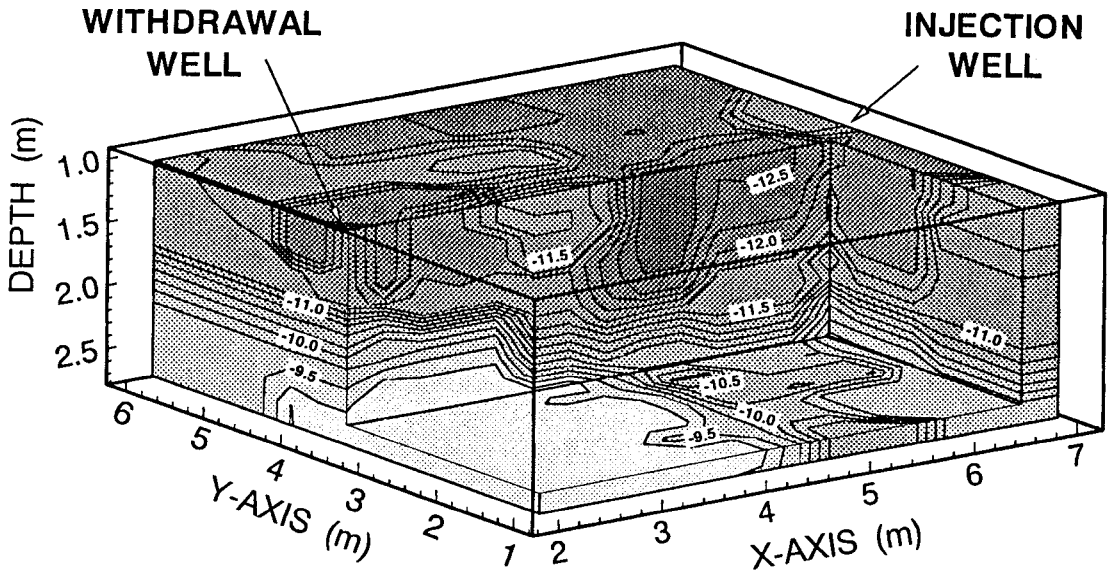

Figure 6. Three-dimensional view of the hydraulic conductivity distribution (based on the H conductivity value set) at the field site. Contour values are expressed in terms of ln K.

aquifer, which is close to the value of 0.3 derived from the analysis of pore structure of intact cores of aquifer materials from one borehole (S. Y. Lee, Oak Ridge National Lab, personal communication, 1994). This porosity value was assumed constant over the entire simulation domain as the variability of porosity is generally considered much smaller than that of the conductivity, and the effect of variation in porosity has been reported to have a minor impact on the flow [*Gelhar et al.*, 1979]. A value of 0.05 m was assigned to the local longitudinal dispersivity, and the local transverse dispersivities were set to 0.015 m. It should be pointed out that since this approach considers the hydraulic conductivity heterogeneity, the spatial variability of hydraulic conductivity plays a much more important role in the transport of solutes than the local dispersivity.

Layered approach. The implementation of the layered approach was similar to the heterogeneous approach described above, but 11 homogeneous layers of 0.15 m thickness were defined. The conductivity value of each layer was assigned as the geometric mean of all measured conductivity values (from the H conductivity value set) at that depth (Table 1). To include the effect of conductivity variability within each layer, neglected by the layer homogeneity assumption, a macrodispersivity concept was employed. However, no theoretical formula relating the variability of conductivity to the dispersivity is available for such a nonuniform flow regime. As initial values, longitudinal and transverse macrodispersivities were estimated by using the result of *Gelhar and Axness* [1983], assuming two-dimensional uniform flow within each layer, with statistically isotropic properties, i.e., $\lambda_1 = \lambda_2 = \lambda$, and $\lambda_3 \to \infty$. According to their formulation the longitudinal and transverse macrodispersivities (A_{11} and A_{22}, respectively) for each layer were calculated by

$$A_{11} = \sigma^2_{\ln K}\lambda/\gamma^2 \tag{4}$$

$$A_{22} = \frac{\sigma^2_{\ln K}\alpha_L}{8\gamma^2}\left[1 + 3\frac{\alpha_T}{\alpha_L}\right] \tag{5}$$

where $\sigma^2_{\ln K}$ is the variance of ln K; λ is the correlation scale of ln K; α_L and α_T are the longitudinal and transverse local dispersivities, respectively; and $\gamma = 1 + \sigma^2_{\ln K}/6$. The statistical parameters for these formulas are given in Table 2 based on the result of the geostatistical analysis presented by Mas-Pla et al. (submitted manuscript, 1995), and the estimated macrodispersivity values are presented in Table 1. These values were input to MMOC3 as the initial estimates of the longitudinal and transverse dispersivities for the simulation. Note that the vertical transverse dispersivity was also set equal to the value of A_{22}. Since, (4) and (5) were derived under the uniform flow condition, which does not represent the flow regime in our forced gradient experiment, the initial dispersivity values were subsequently adjusted by model calibration.

Modeling Approach for August-September 1992 Injection Experiment

The heterogeneous approach using the H conductivity value set was adopted for the simulation of the August-September 1992 injection experiment. The setup of the simulation was identical to that of May 1992 injection experiment, except that boundary conditions for flow simulation were modified to accommodate the influences of the rainfall on the regional gradient (Figure 2) and the additional withdrawal of groundwater from IW 1. Again, an average regional gradient was estimated for the entire duration of the experiment. The effect of the

Table 2. Macrodispersivity Values

Depth, m	$\sigma^2_{\ln K}$	λ, m	A_{11}, m	A_{22}, m
1.15	0.41	0.12	0.05	4×10^{-3}
1.30	0.44	0.12	0.05	4×10^{-3}
1.45	0.44	0.12	0.05	6×10^{-3}
1.60	0.61	0.59	0.31	7×10^{-3}
1.75	0.73	0.59	0.36	8×10^{-3}
1.90	1.01	0.87	0.64	7×10^{-3}
2.05	0.81	0.87	0.57	8×10^{-3}
2.20	0.96	0.27	0.19	8×10^{-3}
2.35	0.92	0.27	0.19	6×10^{-3}
2.50	0.59	0.35	0.18	3×10^{-3}
2.65	0.28	0.35	0.10	4×10^{-3}

variation in withdrawal rate of IW 1 (Figure 4) on the boundary conditions was incorporated in the simulation by assuming an instantaneous steady state flow for each constant pumping period. Head values at the boundary nodes were then estimated by using the Theis solution and a superposition technique for the three active wells with the new regional groundwater gradient. Furthermore, the concentration distribution at the end of each pumping period was used as the initial concentration distribution for the next period.

Moment Analysis

Spatial Moments

The purpose of the spatial moment analysis in this study is to provide a possible criterion to evaluate the performance of our numerical simulation of the May 1992 test. In this moment analysis, simulated concentrations at the eight nodes defining each element were averaged to obtain the concentration within that element. However, concentrations collected at the sampling wells represent point measurements. In addition, sampling wells at the field site do not necessarily coincide with the center of the finite element or nodes. Therefore an interpolation scheme was used to obtain an estimation of the measured concentration at the center of each element so that the density of points used in the moment analysis was the same as that in the simulated result. Data interpolation is a critical step in the process of calculating the spatial moments of the plume. Advantages and disadvantages of several interpolation methods have been discussed in the literature [e.g., *Freyberg*, 1986; *Barry and Sposito*, 1990; *Garabedian et al.*, 1991; *Rajaram and Gelhar*, 1991]. In our analysis we chose a three-dimensional, linear interpolation scheme with inverse distance weights. Because of the layered structure of the aquifer, the vertical lag distance allowed in the interpolation was reduced to one sampling interval (0.3 m), and the interpolation considered the six nearest measurements to the point of interest. This method avoided the negative concentration values generated by higher-order interpolation schemes [*Rajaram and Gelhar*, 1991] and produced a smoothing effect on the discrete data. Although such a smoothing effect is small at the center of the domain, it becomes more critical along its edges where fewer data points are available. To avoid this effect near boundaries, moment calculations were restricted to the square domain of $5 \times 5 \times 1.5$ m which encompassed all the sampling wells but was smaller than the simulation domain.

This moment analysis focused on the zeroth moment, or the total aqueous phase tracer mass within the square domain, and on the first moment, which in this case represents an apparent center of mass because of the truncation of the plume due to the finite spatial extent of the domain. The expression of the zeroth spatial moment is given by

$$M_{000} = \sum_{e=1}^{E} \theta C_e(x, y, z, t) V_e \tag{6}$$

where θ is the porosity, $C_e(x, y, z, t)$ is the concentration at element e, V_e is the volume of that element, and E is the total number of elements within the domain. Coordinates (x, y, z) correspond to the geometric center of each element for which an averaged concentration was estimated.

The first moments, $i + j + k = 1$, are determined by

$$M_{ijk}(t) = \sum_{x_m}^{x_M} \sum_{y_m}^{y_M} \sum_{z_m}^{z_M} \theta C_e(x, y, z, t) x^i y^j z^k V_e \tag{7}$$

where the summations are defined over the minimum and maximum (indicated by subscripts m and M, respectively) coordinates of the $5 \times 5 \times 1.5$ m domain. The center of mass (x_c, y_c, z_c) is then given by

$$x_c = \frac{M_{100}}{M_{000}} \qquad y_c = \frac{M_{010}}{M_{000}} \qquad z_c = \frac{M_{001}}{M_{000}} \tag{8}$$

Temporal Moments

The zeroth and first temporal moments of the observed and simulated breakthrough data at all wells were also analyzed. For a discrete breakthrough curve the zeroth moment, or the breakthrough curve area, is given by

$$t_0 = \sum_{i=1}^{n} C_i \Delta t \tag{9}$$

and the first moment by

$$t_1 = \sum_{i=1}^{n} C_i t_i \Delta t \tag{10}$$

where C_i is the concentration, above background, at location (x, y, z) and at time t_i. Because the observed breakthrough data were sampled at irregular time intervals, a linear interpolation was employed to estimate the concentration values at an equal interval. Both the first and second moments were estimated over the first 100 hours of the breakthrough record (May 1992 test). Finally, the mean arrival time is given by the ratio of the first and the zeroth temporal moments.

Results and Discussion

May 1992 Injection Experiment

Heterogeneous approach. We first consider the heterogeneous approach and then discuss the layered approach.

Head and flow simulations: As mentioned previously, constant head boundary values at the well nodes were adjusted until the simulated injection and withdrawal rates matched those recorded. After the adjustment the difference in the hydraulic heads at the injection and the withdrawal wells was 2.57 m with the H conductivity value set and 1.95 m with the C conductivity value set. These differences cannot be compared with field observations since head levels in the injection and withdrawal wells were not measured during the experiment. However, this simulated head difference is somewhat unrealistic given the actual dimensions of the aquifer. Comparison of observed and simulated head values at other wells of the field site indicated that the result of the numerical simulation exaggerated the head gradient. Such an unrealistic head difference can be attributed to the approximate nature of the estimated hydraulic conductivity data which were estimated by the methods based on simplified assumptions. In fact, a head difference close to the observed could have been reproduced if the values of the H conductivity value set were adjusted (i.e., multiplied by a factor of 3, approximately). However, the hydraulic conductivity values were not adjusted in our simulation because the flow velocity field remained the same regardless of the adjustment.

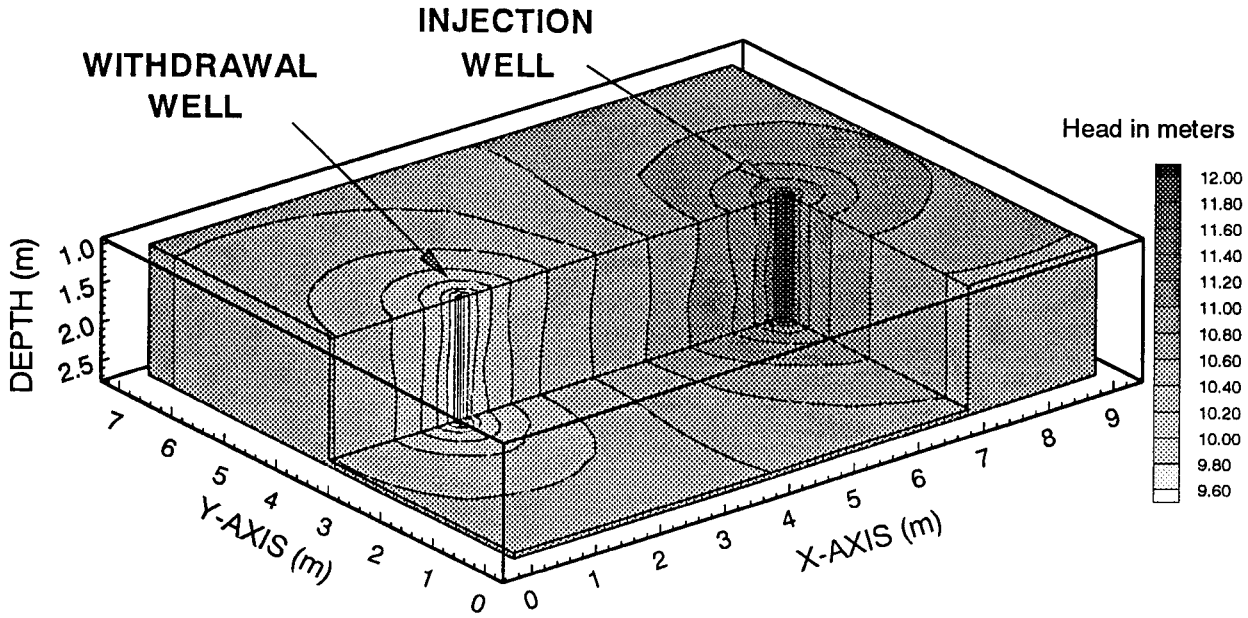

Figure 7. Three-dimensional view of the simulated total head distribution created by the well dipole (using the H conductivity value set).

Figure 7 shows the simulated hydraulic head distribution in three dimensions using the H conductivity value set. Notice that the head equipotential lines are hardly affected by the variation in conductivity even though this variation ranges over more than 1 order of magnitude. The influence of the conductivity variability on the head also seems negligible in the plan views of the head distribution, whereas the effect of regional hydraulic gradient is evident [*Mas-Pla*, 1993]. The velocity field is, however, very sensitive to the hydraulic conductivity variations as shown in Figure 8, where streamlines (using the v_x and v_z components of the velocity vector only) are plotted along the cross section intersecting the injection and withdrawal well. In general, the vertical component of the velocity vector becomes very significant in the areas with drastic changes of conductivity, such as at the center of the site. Consequently, the vertical flow component is more pronounced in the simulation result using the C conductivity value set than the H conductivity value set because of the larger variability produced by the Cooper et al. method of calculation (Mas-Pla et al., submitted manuscript, 1995). Although vertical flow exists, it is generally restricted to contiguous layers. In other words, the hydraulic conductivity distribution at the site does not produce large vertical flows, but rather a broad, layered-flow structure is maintained. Moreover, the layered structure of the hydraulic conductivity distribution has a significant influence on the flux distribution at the wells. Approximately 75% of the total flux was injected through the lowest 0.70 m of the aquifer according to the H data, and 90% was injected according to the C conductivity value set. Similar flux distributions were found at the withdrawal well.

Snapshots of plumes: Figure 9 shows three-dimensional distributions of the observed and simulated chloride plumes (using the H conductivity value set) at 20 hours after injection. It should be pointed out that the distribution of the observed plume illustrated in the figure involved some interpolation and extrapolation owing to the limited size of the sampling network and, consequently, the observed concentration distribution along the y-z (depth) cross section at $x = 7$ m is not shown. In addition, uncertainties in observed concentration exist owing to cross-port contamination and measurement errors. On the other hand, the result of the simulation may include the effect of smoothing of the conductivity field due to the interpolation and the effect of numerical dispersion. In spite of these uncertainties the simulated plumes are generally in good agreement with those observed. A closer comparison between the observed and simulated plumes is given in Figure 10, which depicts behavior of the plumes at several different times in a cross section along a line between the injection and withdrawal wells ($Y = 3.2$ m, see Figure 1). Figure 10 illustrates that simulated results using either the H or the C conductivity value sets represent fairly well the shape of the observed plume. Generally, the movement of the solute is controlled by the layered structure of the conductivity distribution. The fast and slow movements of the solute correspond to the high and low conductivity values at the bottom and top of the aquifer, respectively. At late times (50 hours after the beginning of the chloride injection), this effect of vertical heterogeneity became even more pronounced. The plume was split into two main portions: One part moved through the lower layers, whereas the other part was retained at the upper layers of the aquifer because of the presence of the low-permeability inclusion in the upper central portion of the aquifer (see Figure 6), which enhanced the lateral migration of the plume [*Mas-Pla*, 1993]. As will be discussed later, such a split plume distribution had a major impact on the estimation of the center of mass and consequently suggests that in this case a depth averaging of the plume concentration may be seriously misleading.

Spatial moment estimation: Figure 11a depicts the zeroth moments of the simulated and observed plumes at various times. Generally speaking, the chloride mass calculated on the basis of the simulation using the H conductivity value set agrees well with the mass estimated on the basis of the observed concentration data. In contrast, the simulation using the C conductivity value set produces much lower mass than the observed one. Such a contrast can be imputed to the fact that the mean value of the conductivity of the bottom layer is

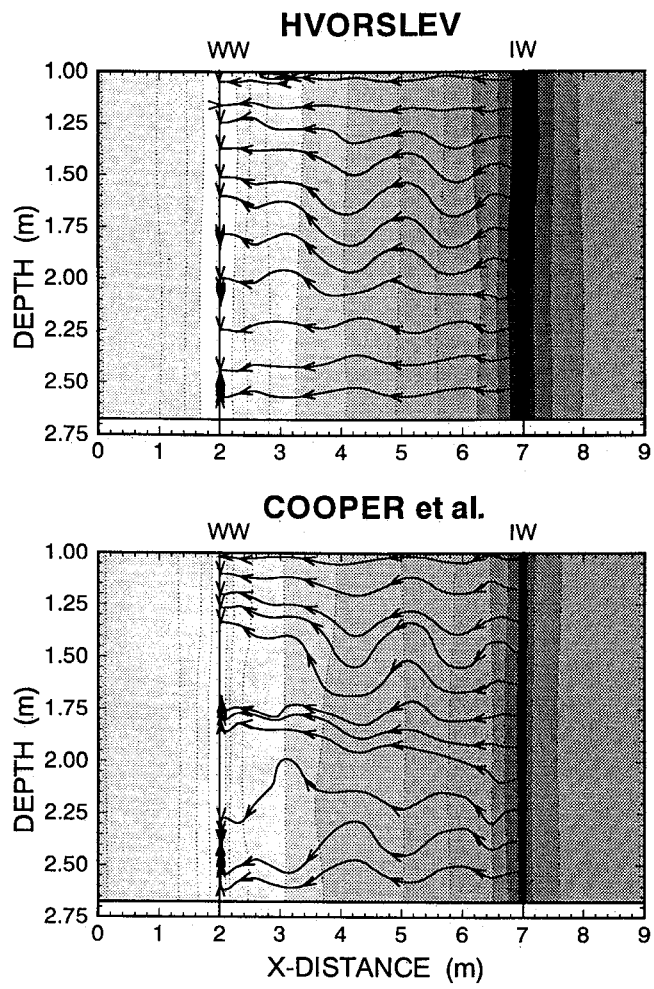

Figure 8. Simulated streamlines produced by the well dipole (using the H conductivity value set) along a cross section between both active wells (IW 2 and WW). Streamlines are generated using only the x and z components of the velocity vector. The distribution of the hydraulic head is also plotted with a contour interval, 0.2 m. Coordinates are the same as in Figure 5.

greater for the C than for the H conductivity value set. Consequently, the simulation using the C conductivity value set produced a much larger amount of chloride moving away from the injection well in the direction opposite of the withdrawal well than that using the H conductivity value set. The mass entering the simulation domain using the C conductivity value set was, thus, considerably less than that using the H conductivity value set. Figure 11a also illustrates that the mass estimated from the observed data is much less than that from the simulation at times greater than 40 hours. This discrepancy can be attributed to the small size of our sampling network and errors introduced by our extrapolation scheme.

Figure 11b shows the movement of the center of mass of the observed and simulated plumes in the x direction as a function of time. In general, the agreement between the simulated and observed plume centers is satisfactory. Note that the injection well is located at $x = 7$ m and the withdrawal well at $x = 2$ m. During the first 20 hours the plume center moved rapidly toward the withdrawal well and slowed down afterward. At times greater than 40 hours the center of mass migrated very slowly away from the center of the experimental site (at $x =$ 4.5 m). The layered structure of the aquifer and the presence of the low-permeability inclusion near the center portion of the experimental site seem responsible for such behavior. At early time, most of the mass moved through the high-permeability bottom layer toward the withdrawal well, resulting in a rapid change in x_c. At the later time a portion of the plume was still retained by the upper zone of low permeability; meanwhile the other portion in the bottom high-permeability zone had already reached the withdrawal well. This resulted in a slowdown in the movement of the center of mass of the plume. At times greater than 40 hours the plume in the upper portion of the aquifer encountered the low-permeability inclusion around $x = 4.5$ m, and the movement of the plume thus became extremely slow.

The plot of the y coordinates of the center of mass of the observed plume, y_c, versus time (Figure 11c) indicates some horizontal drift. Again, the drift of y_c from the central line (the line connecting the injection and withdrawal wells) may be caused by the interpolation scheme and the sampling network. Since wells 2, 8, 16, and 24 had been damaged by the slug tests, the concentration in these areas was underestimated by the interpolation, and the drift of the y_c component is created. However, the variation in the natural hydraulic gradient (Figures 2b and 2c), which was neglected in the simulation, may be partially responsible for this discrepancy.

Finally, the variation of the center of mass of the observed plume along the vertical direction, z_c, is small, and z_c remained approximately constant at 2 m below the ground surface with a tendency to move upward (Figure 11d). This behavior seems consistent with the lithology of the field site. That is, at times earlier than 20 hours the center of mass was close to the bottom high-permeability layer owing to the presence of the large amount of tracer in the layer. After the major portion of the plume reached the withdrawal well through the lower high-permeability zone, the location of the calculated center of mass was merely a reflection of the location of the portion of the plume that remained in the upper low-permeability zone. The tendency of the upward movement of the z_c thus becomes clear.

Breakthrough curves at point sampling ports: Comparisons of the observed and simulated breakthrough data at five different depths of wells 6, 13, 21, and 28 are shown in Figure 12. The simulated and the observed breakthrough data close to the injection well and in the lower layers of the aquifer, which consist of relatively homogeneous material (variance of $\ln K = 0.28$, see Table 1), are in excellent agreement. However, it is difficult to quantitatively evaluate the performance of the simulations using either the H conductivity value set or the C conductivity value set on the basis of this figure. To overcome this difficulty, the temporal moment analysis was applied to the observed and simulated plumes at the five depths of wells 5, 6, 12, 13, 19, 20, 21, 22, 26, 27, 28, and 29 where breakthrough data were available. Comparisons of the temporal moments (area and arrival time) of observed and simulated breakthroughs are illustrated in Figures 13a–13d. The areas under the simulated breakthrough curves using the H and the C conductivity value sets at different depths and wells are plotted in Figures 13a and 13b, respectively, against the areas from the observed data. The areas of the simulated breakthroughs using the H conductivity value set are, on the average, greater than those estimated on the basis of the observed data (Figure 13a). On the other hand, the areas of the simulated breakthrough using the C conductivity value set tend to be smaller than those

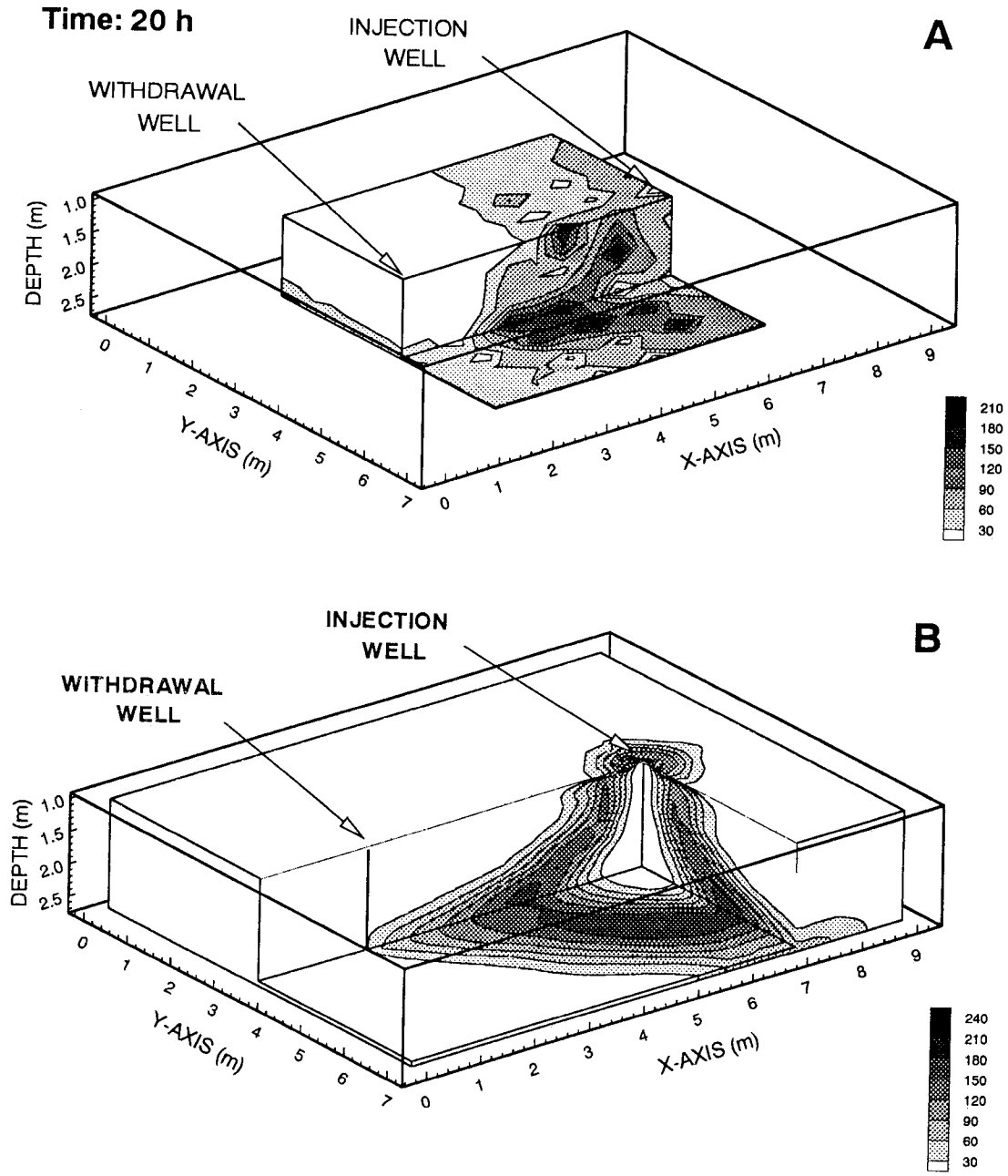

Figure 9. Three-dimensional views of the (a) observed and (b) simulated chloride concentrations at time 20 hours at the May 1992 test (using the H conductivity value set).

of the observed data (Figure 13b). However, the areas of the simulated breakthroughs at the lower portion of the aquifer using either the H or the C conductivity value set agree well with those observed.

The arrival times of the center of mass of the simulated breakthroughs using the H and the C conductivity value sets are compared against those of the observed breakthroughs in Figures 13c and 13d, respectively. The arrival times of the observed breakthroughs are better reproduced by the simulation using the H conductivity value set than the C set. Again, the agreement between the simulation and observation is excellent for the bottom layers (the layers at 2.0, 2.3, and 2.6 m) and becomes progressively worse as depth decreases. The factors producing the large discrepancies between the simulation and the observation near the land surface include, in addition to the high heterogeneity of the soil, the incorrect representation of the water table condition, as well as measurement errors in hydraulic conductivity or concentration at these upper layers. Furthermore, the flat chloride breakthroughs observed at the sampling ports at the upper layers far from the injection well (see Figure 12) make the estimation of the first moment highly inaccurate. Overall, the simulation based on the H conductivity value set reproduces the observed data better than that based on the C conductivity value set.

Breakthrough curve at the withdrawal well: Simulated breakthrough curves at the withdrawal well are shown in Figure 14 and were obtained by averaging the concentrations at the well nodes using nodal fluxes as weights. As demonstrated in the figure, the breakthrough curve resulting from the H conductivity value set successfully reproduced the observed

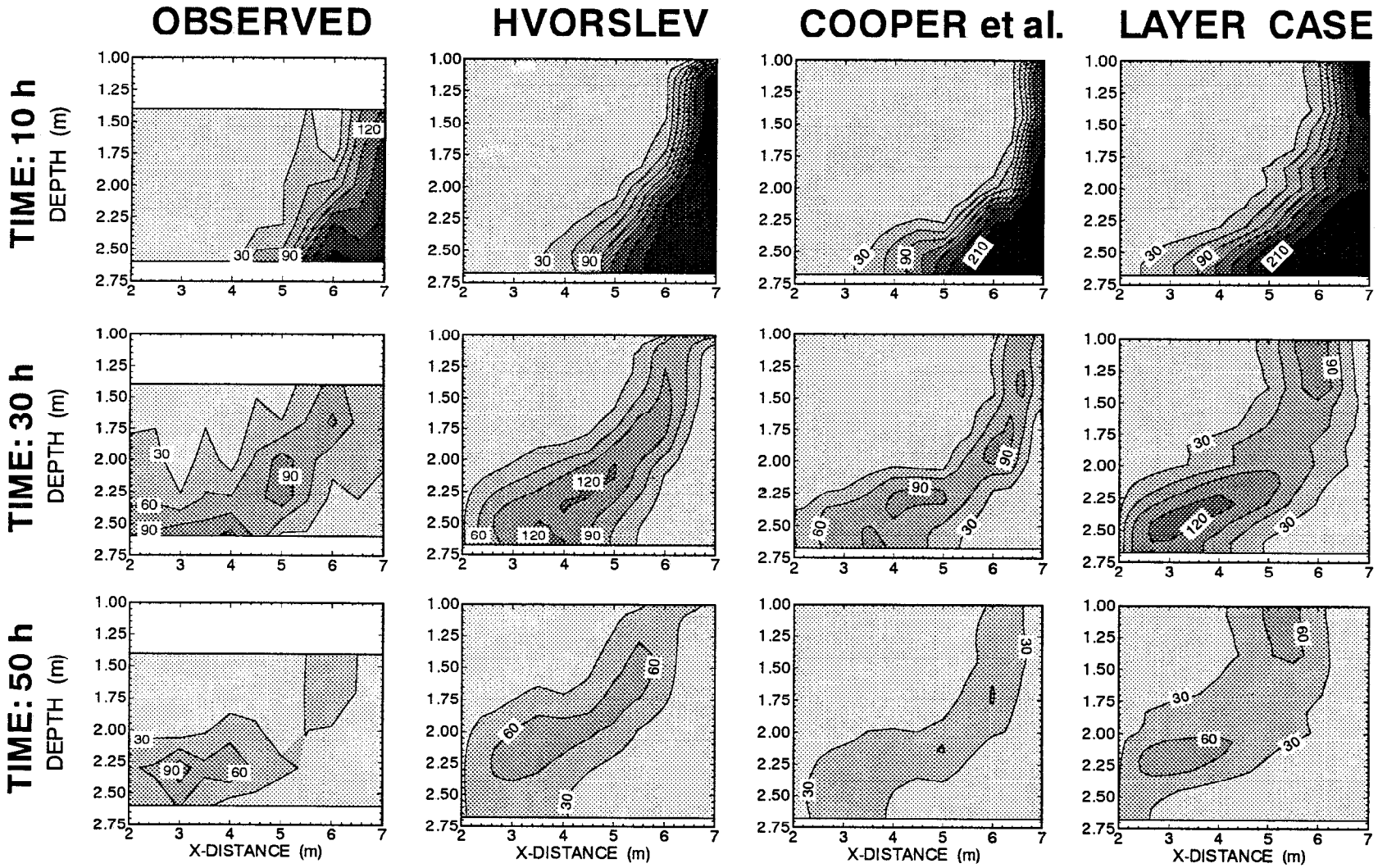

Figure 10. Observed and simulated chloride distribution in a cross section along the coordinate $Y = 3.2$ m (May 1992 test). Concentration contour interval is 30 mg/L. Coordinates are the same as in Figure 5.

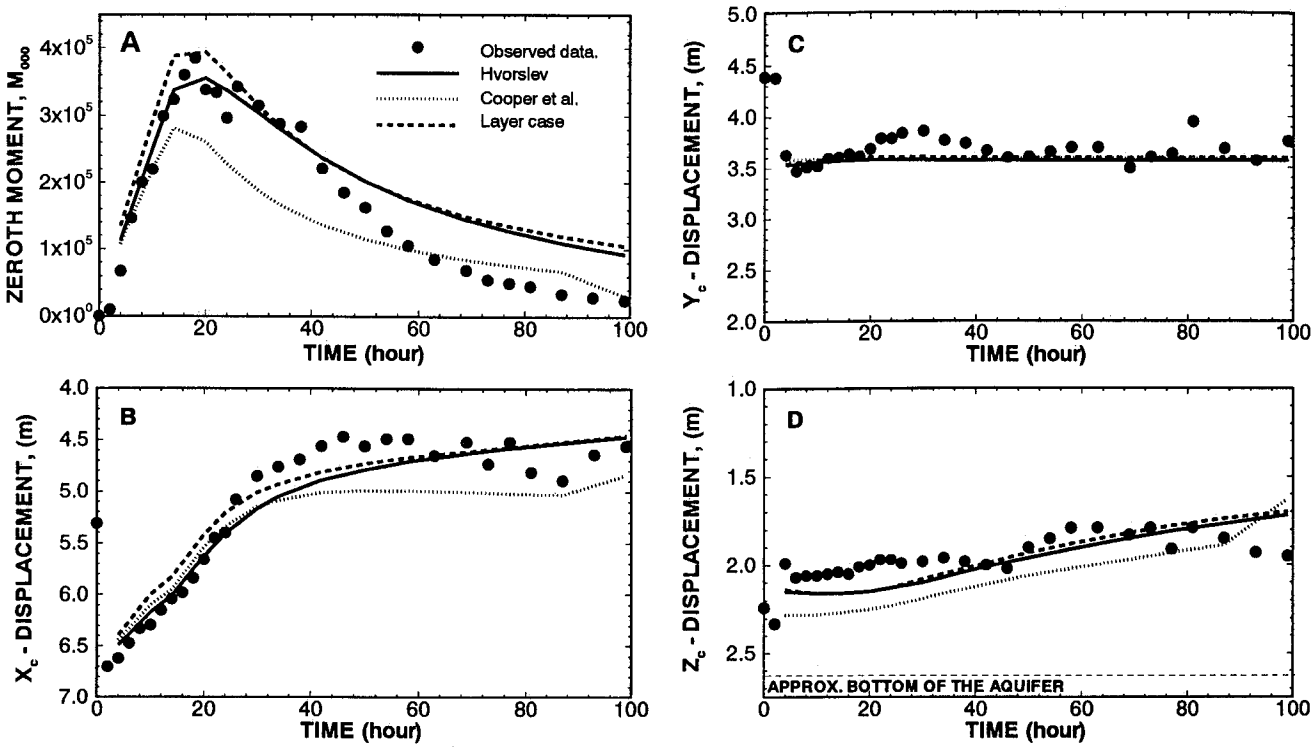

Figure 11. Spatial moment analysis of the observed and simulated chloride plumes (May 1992 test). (a) Zeroth moment, or total mass versus time. (b, c, d) Location of the components of the center of mass (x_c, y_c, and z_c in Figures 11b, 11c, and 11d, respectively) versus time. Injection well is located at coordinates (7.0, 3.5), and the withdrawal well at coordinates (2.0 m, 3.5 m). Coordinates are consistent with Figure 5.

data. Conversely, the simulation based on the C conductivity value set predicted an earlier chloride breakthrough at the withdrawal well and underestimated the tail of the observed breakthrough. The early arrival of the chloride peak is attributed to the large values of the hydraulic conductivity estimated by the Cooper et al. method for the lower layers of the aquifer.

The layered approach. As mentioned in the modeling approach, there is no explicit methodology to estimate the dispersivity values to account for the variation in conductivity within each layer when the heterogeneous layer is assumed homogeneous. The initial estimates for these parameters were based on formulae for uniform flow developed by *Gelhar and Axness* [1983]. Owing to unsatisfactory simulation results using the initial values (Figure 14, case $A_{11} \neq A_{22}$), the transverse (vertical and horizontal) dispersivity values were adjusted to be equal to the longitudinal dispersivity (i.e., $A_{11} = A_{22}$), resulting in a better agreement between the observed and the simulated breakthrough at the withdrawal well (Figure 14, case $A_{11} = A_{22}$). The following discussion is based on the results of the simulation after such a calibration.

The simulated chloride distributions, using the layered approach, at different times along the cross section are depicted in Figure 10. This figure shows that the use of the macrodispersion concept results in a greater spread of the plume as compared with the observed plume distribution and the simulated plume distribution based on the full heterogeneity approach. However, the general shape of the simulated plume based on the layered approach is similar to that of the observed one.

Figure 11 presents the evolution of the zeroth moment and the location of the center of mass of the plume as a function of time. In general, they agreed well with those simulated by the heterogeneous approach. Such an agreement indicates that these two moments, spatially integrated measurements, cannot distinguish the difference in the plume distributions resulting from heterogeneities below the scale of the layer.

Figure 12 compares the observed and simulated breakthrough curves based on the heterogeneous and layered approaches at wells 28, 21, 13, and 6 at five different depths. The peak arrival times of the simulated breakthrough curves near the bottom of the aquifer generally agree well with those observed, but the peak concentrations were greatly underestimated by the layered approach, even compared with those obtained by the simulation based on the H conductivity value set. At the upper portion of the aquifer, the agreement between the simulated breakthrough curves based on the layered approach becomes even worse.

Such discrepancies between the observed and simulated breakthrough curves at the small sampling ports are expected because the predicted concentration distribution represents an ensemble average concentration for the given layer (i.e., the average concentration resulting from many possible heterogeneities of the layer), which does not necessarily correspond to that of a single realization [e.g., *Yeh*, 1992]. This is one of the reasons that the temporal moment analysis was not carried out for the layered case. However, theoretically, the breakthrough at the withdrawal well, which integrates the contribution from many different parts of the aquifer, will be close to the ensemble concentration. As depicted in Figure 14, the chloride breakthrough at the withdrawal well was fairly well reproduced by the layered model, but it is still not as good as those based on the heterogeneous approach. More importantly, the mac-

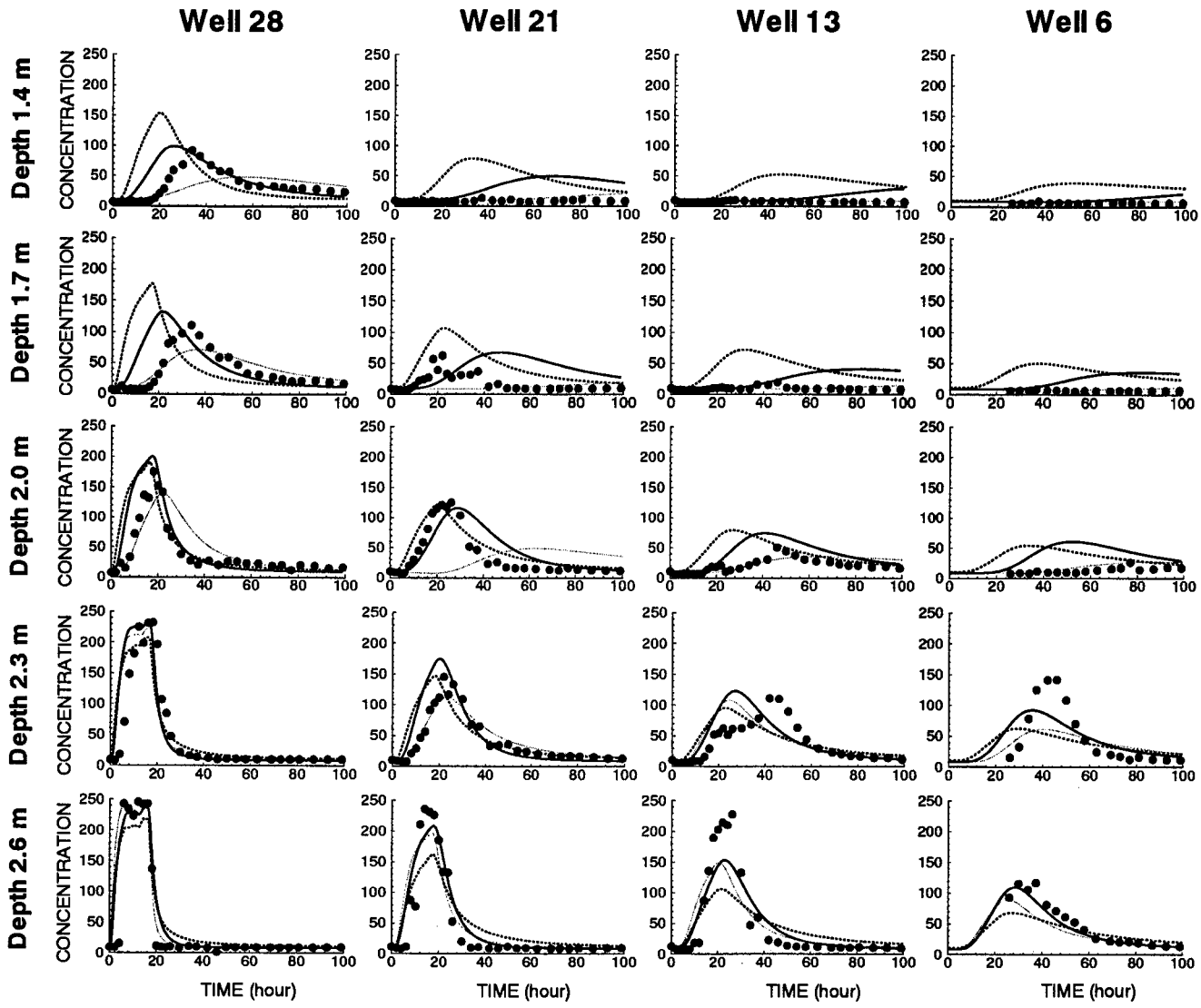

Figure 12. Observed and simulated chloride breakthrough curves at wells 6, 13, 21, and 28 (May 1992 test). Solid circles denote observed data; solid line denotes H conductivity value set simulation; dotted line denotes C conductivity value set simulation; and dashed line denotes layer case.

rodispersivity values must be adjusted in order to produce a reasonable agreement between the observed and simulated breakthroughs.

August-September 1992 Injection Experiments

As demonstrated in the simulations of the May 1992 tracer test, it is evident that the heterogeneous approach can reproduce the groundwater velocity field at the field site with reasonable accuracy and is superior to the layered approach. Also the H conductivity value set yields more satisfactory results than the C conductivity value set. On the basis of these results, the simulation of August-September 1992 experiments was, therefore, conducted using the fully three-dimensional heterogeneous approach with the conductivity values estimated by the Hvorslev method.

The observed and simulated chloride concentration distributions along the cross section in between the injection and withdrawal wells at different times are illustrated in Figure 15. A comparison of these distributions clearly shows that the result of the simulation is not as successful as in the May 1992 experiment. In general, the simulated plume moves faster than the observed one, although the patterns are very similar. The discrepancies between the observed and the simulated plumes become very significant at time equal to 84 hours and after. Similar to the result of the simulation of the May 1992 experiment, the greatest discrepancies occur in the upper layers. Such significant discrepancies are likely caused by our incorrect representation of the changes in boundary conditions as a result of rainfall events, in addition to those factors discussed in the simulation of the May 1992 experiment. Also, our simplified quasi-steady state approach for tackling the effect of pumping of the second withdrawal well may augment these discrepancies. Consequently, our simulation overestimated the flow rate of the entire aquifer.

Nevertheless, Figure 16 shows that the agreement between the simulated and the observed breakthroughs at wells 28, 21, 13, and 6 at the bottom of the aquifer (depth 2.6 m) is excellent up to approximately 300 hours before the effect of rainfall events and the additional pumping becomes significant in the lower portion of the aquifer. A similar agreement was observed

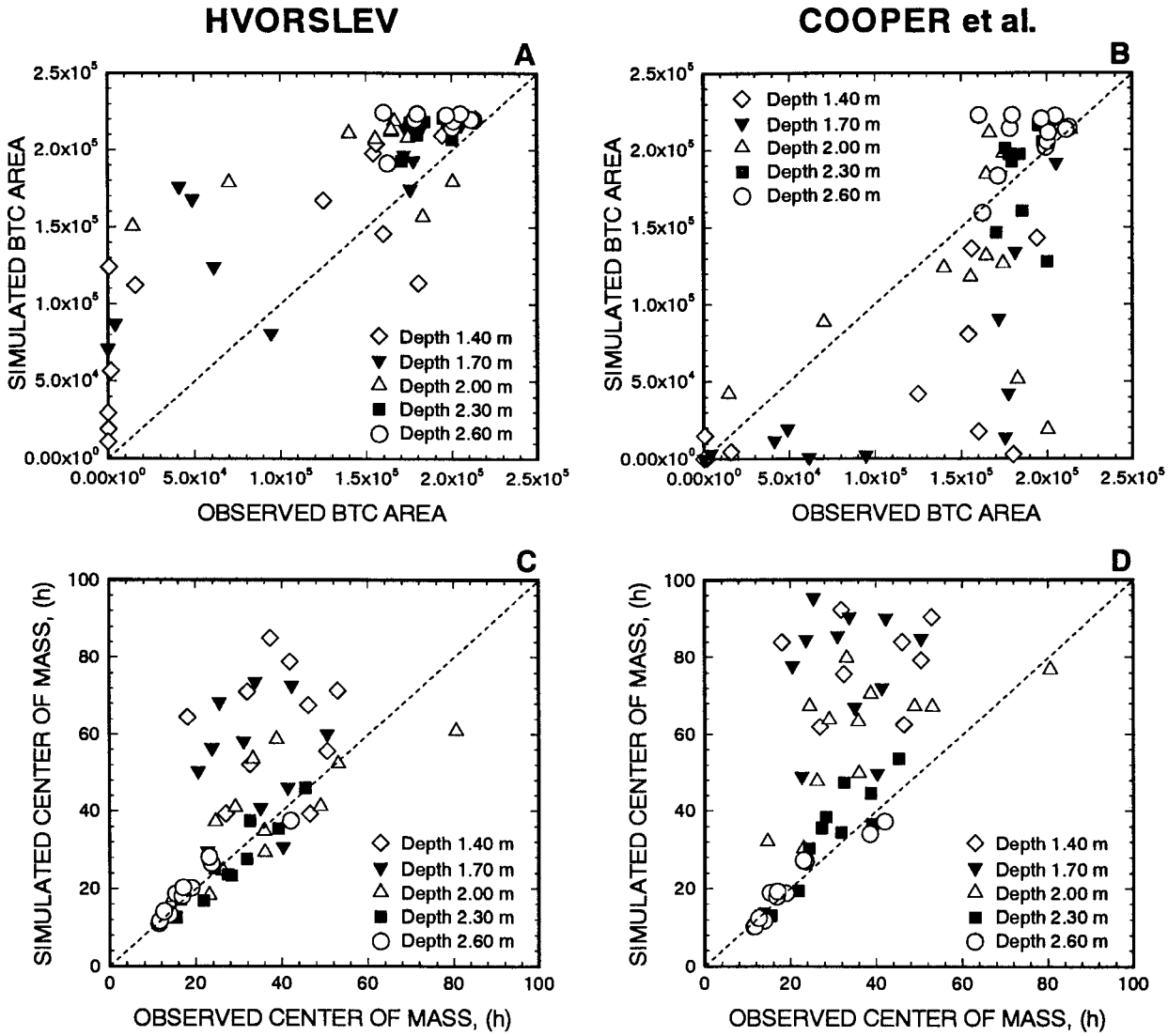

Figure 13. Comparison of the observed and simulated areas and centers of mass (mean arrival time) of the breakthrough curves at all sampling ports at wells 5, 6, 12, 13, 19, 20, 21, 22, 26, 27, 28, and 29 where data were collected (May 1992 test). Areas are in units of milligrams per liter times minutes.

at the withdrawal well (Figure 17). Notice that the small discrepancy between the simulated and observed peak arrival times corresponds to a time span of several hours, which is very significant because of the short distance between the injection and withdrawal wells.

Conclusions

Two-well, forced-gradient tracer experiments and three-dimensional simulations of the transport of chloride tracer plumes in a coastal, sandy aquifer in Georgetown, South Carolina, were conducted in an attempt to isolate effects of hydrological heterogeneities from mechanisms of NOM transport. Three-dimensional hydraulic conductivity value sets, derived using both the Hvorslev method and the method of Cooper et al. from the slug test data, were employed in the simulations. A

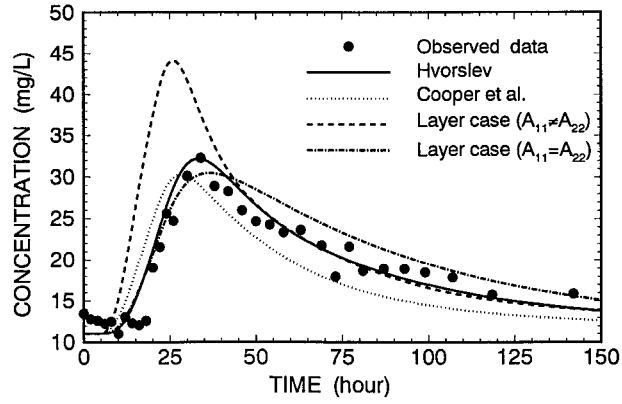

Figure 14. Observed and simulated chloride breakthrough curves at the withdrawal well (May 1992 test).

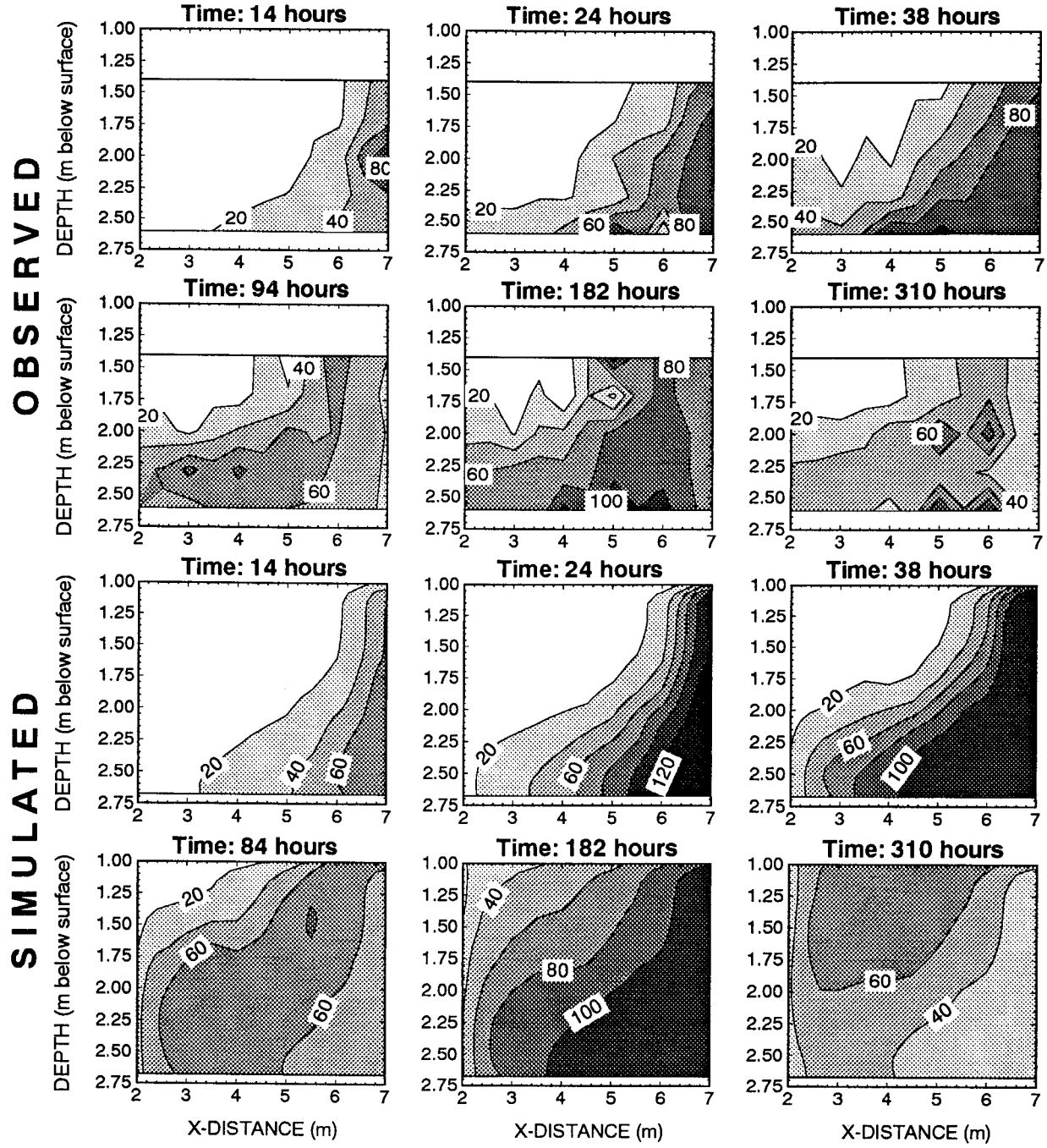

Figure 15. Observed and simulated chloride distribution (using H conductivity value set) in a cross section along the coordinate $Y = 3.2$ m (August-September 1992 test). Concentrations are given in milligrams per liter, and contour interval is 20 mg/L. Coordinates are consistent with Figure 5.

heterogeneous approach and a layered approach were tested. The heterogeneous approach with hydraulic conductivity values determined by the Hvorslev method most adequately reproduced the main features of the observed chloride plume in the May experiment. Prediction was best for integrated measures of plume behavior, moments or concentrations at the withdrawal well. Behavior at individual sampling ports was well predicted only near the injection well and in the lower, more homogeneous zone. This result agrees with the finding by *Molz et al.* [1986] that the breakthrough at the withdrawal well (an integrated behavior of the plume) is predictable if sufficient geological information is available. The results of our study also suggest that measurement errors in slug tests, uncertainties in the interpretation of slug test results, errors in interpolation of conductivity values to finite elements, and difficulties in controlling numerical dispersion in the simulation, etc., make predictions of detailed plume behaviors (such as concentration breakthroughs at small sampling ports) in aquifers highly questionable, even if many hydraulic conductivity measurements are available.

On the basis of our observations and simulations, it can also be concluded that the bulk behavior of the plume is mainly controlled by a few "significant" heterogeneities, namely, the aquifer stratification and the low-permeability inclusion be-

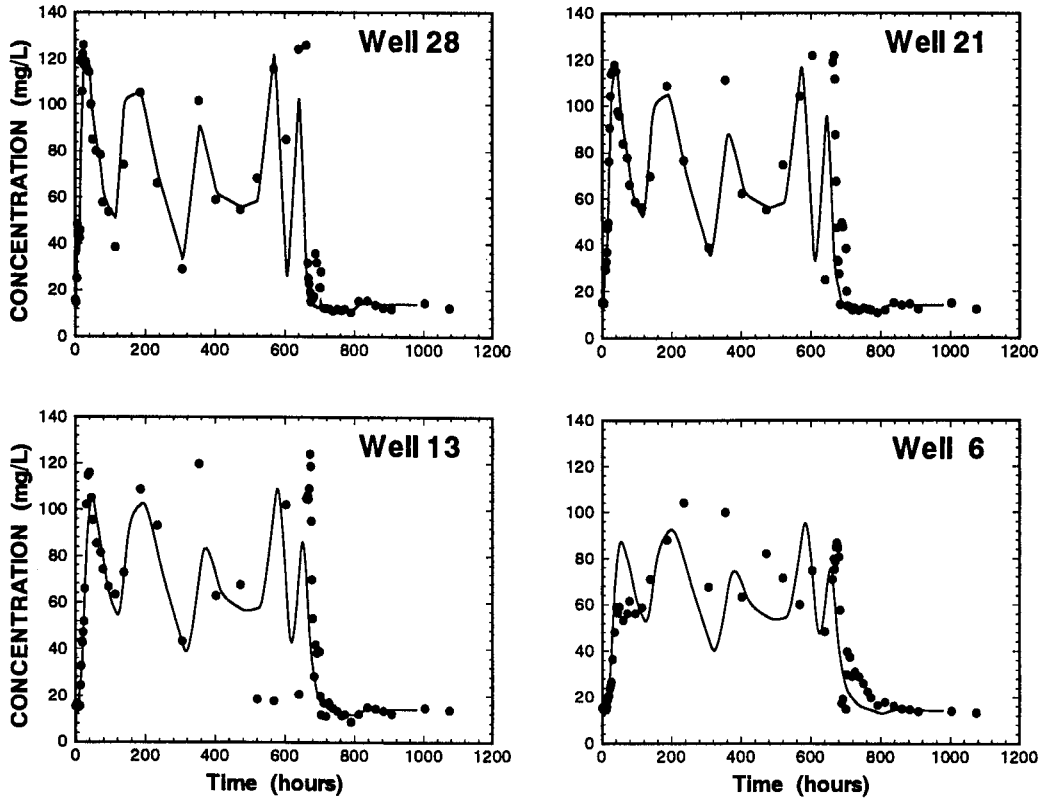

Figure 16. Chloride breakthrough curves at depth 2.6 m at wells 6, 13, 21, and 28 (August-September 1992 test).

tween the injection and the withdrawal wells. The contrast in the results of our layered and heterogeneous approaches supports this conclusion. Nonetheless, a large number of hydraulic conductivity measurements were necessary in order to identify these "significant" heterogeneities.

Although the general trend of the spatial distribution of the conductivity values derived from the Hvorslev method and the method by Cooper et al. is similar, our numerical simulation results show that the conductivity data set based on the Hvorslev method yielded more acceptable plume distributions, breakthrough curves at the withdrawal well, and temporal and spatial moments. The variability of ln K estimated from the data set derived from Hvorslev's method is in better agreement with data from aquifers of similar depositional environments [*Garabedian et al.*, 1991]. Nevertheless, even using these values, the head values at the injection and the withdrawal wells had to be adjusted by allowing unrealistic values for gradient. The results of this study do agree with numerical simulation evaluations of *Butler et al.* [1994] that the Cooper method is more applicable to slug tests with a large aspect ratio. The slug tests in this study, with an aspect ratio of 12, seem more accurately evaluated by the Hvorslev method. As one tries to finely resolve conductivity of a given aquifer thickness with multilevel slug tests, the aspect ratio will necessarily decline, and the Hvorslev method will become more appropriate.

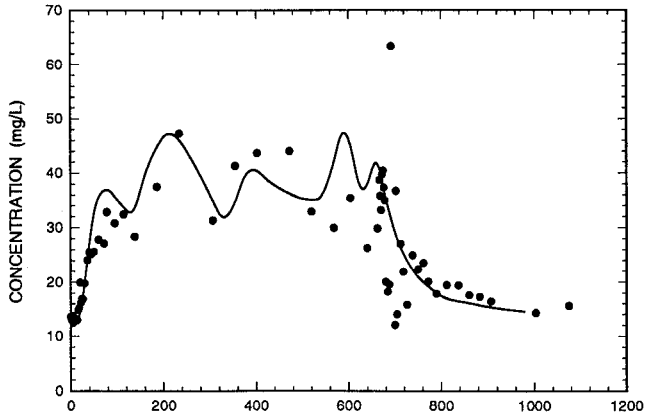

Figure 17. Observed and simulated chloride breakthrough curves at the withdrawal well (August-September 1992 test).

For predicting the zeroth and first moments of the plume and an integrated concentration distribution (such as the breakthrough at the fully screened withdrawal well), the layered approach with calibrated macrodispersivity values was acceptable, but it did not reproduce the plume distribution as satisfactorily as the fully heterogeneous approach. A matter of greater concern was the lack of an explicit method for estimating the macrodispersivity values under such a nonuniform flow regime. Hence a trial-and-error procedure had to be used in the layered approach to obtain a reasonable fit to the observed chloride data. The results of our simulation of the tracer test conducted during August and September 1992 illustrate the importance of temporal variability in boundary conditions in addition to the spatial variability of hydrologic properties of the aquifer. For predicting long-term transport of contaminants in aquifers, one must also consider temporal variability of boundary conditions, which has been neglected in the past.

Despite our inability to model concentration distributions at all points within the aquifer, the concentration breakthrough

curves within the lower "more conductive and less variable" layer were adequately modeled in both May and August-September experiments. The bulk behavior of both the plume and breakthrough from these accurately modeled points can be used to interpret chemical behavior of NOM in the August-September experiment.

Acknowledgments. The authors are grateful for the long and hard work of the dedicated team of investigators and technicians from Oak Ridge National Laboratory and Clemson University who collected all the data described in this paper, including Baohua Gu, Louwanda Jolley, Liyuan Liang, Charles McCutcheon, Jennifer McDonald, Tonia Mehlhorn, John Paulk, and William Sanford. This research was supported by the Subsurface Science Program, Environmental Sciences Division, U.S. Department of Energy, under Contract DE-AC05-84OR21400 with Martin Marietta Energy Systems, Inc., and grant DE-FG02-91ER61199. J. Mas-Pla was also supported by "Fundació La Caixa" (Barcelona, Spain). Support from NSF grant EAR-9317009 and NIEHS grant ES04949 is also acknowledged.

References

Barry, D. A., and G. Sposito, Three-dimensional statistical moment analysis of the Stanford/Waterloo Borden tracer data, *Water Resour. Res.*, *26*(8), 1735–1747, 1990.

Butler, J. J., G. C. Bohling, Z. Hyder, and C. D. McElwee, The use of slug tests to describe vertical variations in hydraulic conductivity, *J. Hydrol.*, *156*, 137–162, 1994.

Cooper, H. H., Jr., J. D. Bredehoeft, and I. S. Papadopulos, Response of a finite diameter well to an instantaneous charge of water, *Water Resour. Res.*, *3*(1), 263–269, 1967.

Dagan, G., Theory of solute transport by groundwater, *Annu. Rev. Fluid Mech.*, *19*, 183–215, 1987.

Freyberg, D. L., A natural gradient experiment on solute transport in a sand aquifer, 2, Spatial moments and the advection and dispersion of nonreactive tracers, *Water Resour. Res.*, *22*(13), 2031–2046, 1986.

Garabedian, S. P., D. R. LeBlanc, L. W. Gelhar, and M. A. Celia, Large-scale natural gradient tracer test in sand and gravel, Cape Cod, Massachusetts, 2, Analysis of spatial moments for a nonreactive tracer, *Water Resour. Res.*, *27*(5), 911–924, 1991.

Gelhar, L. W., *Stochastic Subsurface Hydrology*, 390 pp., Prentice-Hall, Englewood Cliffs, N. J., 1993.

Gelhar, L. W., and C. L. Axness, Three-dimensional stochastic analysis of macrodispersion in aquifers, *Water Resour. Res.*, *19*(1), 161–180, 1983.

Gelhar, L. W., A. L. Gutjahr, and R. L. Naff, Stochastic analysis of macrodispersion in a stratified aquifer, *Water Resour. Res.*, *15*(6), 1387–1397, 1979.

Greenberg, A. E., R. R. Trussell, and L. C. Clesceri, *Standard Methods for Examination of Water and Waste Water*, Am. Publ. Health Assoc., Washington, D. C., 1985.

Güven, O., F. J. Molz, J. G. Melville, S. El Didy, and G. K. Boman, Three-dimensional modeling of a two-well tracer test, *Ground Water*, *30*(6), 945–957, 1992.

Huyakorn, P. S., P. F. Anderson, O. Güven, and F. J. Molz, A curvilinear finite element model for simulating two-well tracer tests and transport in stratified aquifers, *Water Resour. Res.*, *22*(5), 663–678, 1986.

Hvorslev, M. J., Time lag and soil permeability in groundwater observations, *Waterw. Exp. Stn. Bull. 36*, 50 pp., U.S. Army Corps of Eng., Vicksburg, Miss., 1951.

Jensen, K. H., K. Bitsch, and P. L. Bjerg, Large-scale dispersion experiments in a sandy aquifer in Denmark: Observed tracer movements and numerical analyses, *Water Resour. Res.*, *29*(3), 673–696, 1993.

Mas-Pla, J., Modeling the transport of natural organic matter in heterogeneous porous media: Analysis of a field-scale experiment at the Georgetown site, SC, Ph.D. dissertation, Univ. of Ariz., Tucson, 1993.

Mas-Pla, J., T.-C. J. Yeh, T. M. Williams, and J. F. McCarthy, A forced gradient tracer experiment in a coastal sandy aquifer, Georgetown site, South Carolina, *Ground Water*, *30*(6), 958–964, 1992.

Molz, F. J., O. Güven, J. G. Melville, R. D. Crocker, and K. T. Matteson, Performance, analysis, and simulation of a two-well tracer test at the Mobile site, *Water Resour. Res.*, *22*(7), 1031–1037, 1986.

Molz, F. J., O. Güven, J. G. Melville, J. S. Nohrstedt, and J. K. Overholtzer, Forced-gradient tracer tests and inferred hydraulic conductivity distribution at the Mobile site, *Ground Water*, *26*(5), 570–579, 1988.

Pickens, J. F., and G. E. Grisak, Scale-dependent dispersion in a stratified granular aquifer, *Water Resour. Res.*, *17*(4), 1191–1211, 1981.

Rajaram, H., and L. W. Gelhar, Three-dimensional spatial moment analysis of the Borden test site, *Water Resour. Res.*, *27*(6), 1239–1251, 1991.

Rehfeldt, K. R., J. M. Boggs, and L. W. Gelhar, Field study of dispersion in a heterogeneous aquifer, 3, Geostatistical analysis of hydraulic conductivity, *Water Resour. Res.*, *28*(12), 3309–3324, 1992.

Srivastava, R., and T.-C. J. Yeh, A three-dimensional numerical model for water flow and transport of chemically reactive solute through porous media under variably saturated conditions, *Adv. Water Resour.*, *15*(5), 275–287, 1992.

Sudicky, E., A natural gradient experiment on solute transport in a sand aquifer: Spatial variability of hydraulic conductivity and its role in the dispersion process, *Water Resour. Res.*, *22*(13), 2069–2082, 1986.

Williams, T. M., and J. F. McCarthy, Field-scale tests of colloids: Facilitated transport, paper presented at National Research and Development Conference on the Control of Hazardous Materials, Hazardous Mater. Control Res. Inst., Anaheim, Calif., Feb. 20–22, 1991.

Yeh, T.-C. J., Stochastic modeling of groundwater flow and solute transport in aquifers, *J. Hydrol. Processes*, *6*, 369–395, 1992.

Yeh, T.-C. J., R. Srivastava, A. Guzmán, and T. Harter, A numerical simulation for water flow and chemical transport in variably saturated porous media, *Ground Water*, *31*(4), 634–644, 1993.

J. Mas-Pla, Unitat de Geodinàmica Externa i Hidrogeologia, Departamento de Geologia, Universitat Autònoma de Barcelona, 08193 Bellaterra, Spain.

J. F. McCarthy, Environmental Science Division, Oak Ridge National Laboratory, P. O. Box 2008, Oak Ridge, TN 37831.

T. M. Williams, College of Forest and Recreation Resources, Belle W. Baruch Forest Science Institute, Clemson University, Georgetown, SC 29442.

T.-C. J. Yeh, Department of Hydrology and Water Resources, University of Arizona, Tucson, AZ 85721.

(Received August 31, 1994; revised June 22, 1995;
accepted June 22, 1995.)